Follow us @BoneJointRes

Freely available online OPEN ACCESS

BJR

ARTHRITIS

ATF3 as a potential diagnostic marker of early-stage osteoarthritis and its correlation with immune infiltration through bioinformatics analysis

J. Yang,
Y. Fan,
S. Liu

From Peking Union Medical College Hospital, Chinese Academy of Medical Science, Beijing, China

Aims

This study aimed, through bioinformatics analysis, to identify the potential diagnostic markers of osteoarthritis, and analyze the role of immune infiltration in synovial tissue.

Methods

The gene expression profiles were downloaded from the Gene Expression Omnibus (GEO) database. The differentially expressed genes (DEGs) were identified by R software. Functional enrichment analyses were performed and protein-protein interaction networks (PPI) were constructed. Then the hub genes were screened. Biomarkers with high value for the diagnosis of early osteoarthritis (OA) were validated by GEO datasets. Finally, the CIBERSORT algorithm was used to evaluate the immune infiltration between early-stage OA and end-stage OA, and the correlation between the diagnostic marker and infiltrating immune cells was analyzed.

Results

A total of 88 DEGs were identified. Gene ontology (GO) and Kyoto Encyclopedia of Genes and Genomes (KEGG) enrichment analyses indicated that DEGs were significantly enriched in leucocyte migration and interleukin (IL)-17 signalling pathways. Disease ontology (DO) indicated that DEGs were mostly enriched in rheumatoid arthritis. Six hub genes including FosB proto-oncogene, AP-1 transcription factor subunit (FOSB); C-X-C motif chemokine ligand 2 (CXCL2); CXCL8; IL-6; Jun proto-oncogene, AP-1 transcription factor subunit (JUN); and Activating transcription factor 3 (ATF3) were identified and verified by GEO datasets. ATF3 (area under the curve = 0.975) turned out to be a potential biomarker for the diagnosis of early OA. Several infiltrating immune cells varied significantly between early-stage OA and end-stage OA, such as resting NK cells ($p = 0.016$), resting dendritic cells ($p = 0.043$), and plasma cells ($p = 0.043$). Additionally, ATF3 was significantly correlated with resting NK cells ($p = 0.034$), resting dendritic cells ($p = 0.026$), and regulatory T cells (Tregs, $p = 0.018$).

Conclusion

ATF3 may be a potential diagnostic marker for early diagnosis and treatment of OA, and immune cell infiltration provides new perspectives for understanding the mechanism during OA progression.

Cite this article: *Bone Joint Res* 2022;11(9):679–689.

Keywords: Early osteoarthritis, Immune infiltration, Synovial tissue, Bioinformatics analysis, Differentially expressed genes

Article focus

- How can we diagnose and treat osteoarthritis (OA) at the early stage?
- What is the relationship between OA and immune cell infiltration?
- What is the significance of this relationship to the treatment of OA?

Key messages

- Activating transcription factor 3 (ATF3) can be a potential diagnostic marker and therapeutic target for early-stage OA.
- Immune cell infiltration is of great significance in the development of OA.

Correspondence should be sent to Yu Fan; email: fanyu1979@live.cn

doi: 10.1302/2046-3758.119.BJR-2022-0075.R1

Bone Joint Res 2022;11(9):679–689.

Strengths and limitations

- The present study revealed that ATF3 could be a potential diagnostic marker and therapeutic target for early-stage OA, and we associated ATF3 with immune cell infiltration in OA to elucidate its role in the development of the disease.
- Experimental verification and a large-scale sample size are still needed for better reliability of the results in the future.

Introduction

Osteoarthritis (OA) is the most common chronic degenerative joint disease which is mainly characterized by synovial inflammation and cartilage degeneration among older people.[1,2] OA can cause serious limits on articular functions in major daily activities without an effective treatment.[3] Over 200 million people worldwide suffer from OA, which is a great burden both for individuals and for society.[4] However, early diagnosis and treatment are imperative to effectively prevent disease progression and joint damage.[5] Currently, diagnosis is based on clinical manifestations and imaging, which can only detect quite advanced OA. Moreover, the severity of structural degeneration and clinical manifestations are not consistent.[6] The lack of reliable methods to diagnose, stage, and monitor pathological changes in the joint has been one of the major impediments to advances in disease-modifying interventions.[7] Therefore, it is essential to identify new and effective biomarkers for the early diagnosis and treatment of OA.

OA has now been recognized as a disease that affects whole-joint tissues, including the synovium (synovial tissue), which can produce synovial fluid and maintain the smoothness and motion of the joint. Some studies indicate that the pathological changes in synovium occur even before visible cartilage degeneration in OA.[8] Multiple findings from MRI and ultrasound techniques have confirmed the existence of synovial pathological changes, such as thickening of the synovial lining layer and joint effusion, in early OA.[9,10] With the onset of synovitis, proinflammatory cytokines produced by inflamed synovial tissue cause the cartilage breakdown which can, in turn, exacerbate synovitis, creating a vicious circle.[11] However, only a few pieces of research focus on exploring the molecular mechanism between synovitis and the progression of OA. An increasing number of studies have demonstrated that cell infiltration plays a crucial role in the development of OA.[12] Numerous immune cells have been discovered in the synovial tissue of OA patients. Among them, macrophages, T cells, and mast cells (MCs) are the most frequently identified infiltrating immune cells.[13] In addition, a distinct infiltration pattern characterized by the increasing polarization of $CD4^+$ T cells towards activated Th1 cells, and the increased secretion of immunomodulating cytokines, was recently discovered.[14] Therefore, understanding infiltration of the immune cells is of great importance to elucidate the mechanisms of OA, while identifying the differences in components of infiltrating immune cells is beneficial to the development of new immunotherapeutic targets. However, no studies have yet analyzed the difference in immune cell infiltration between early-stage OA and end-stage OA.

Methods

Microarray datasets collection and preprocessing. We used the "GEOquery" package of R software (version 4.1.1, R Foundation for Statistical Computing, Austria) to download gene expression profiles of human synovial tissues, including three test sets GSE55235, GSE55457, and GSE55584 based on GPL96 platforms, and two validation sets including GSE12021 based on GPL96 platforms, and GSE32317 based on GPL570 platforms from the GEO database.[15] Three test sets GSE55235, GSE55457, and GSE55584 contain 46 samples, including 20 normal samples and 26 OA samples. GSE12021 contains 19 samples, including nine normal samples and ten OA samples (Table I). GSE32317 contains 19 samples, including nine end-stage OA samples and ten early-stage OA samples. GSE55235, GSE55457, and GSE55584 gene expression matrixes were then combined, and the "sva" package was used to remove the inter-batch difference and other unwanted variations.[16]

Identification of DEGs. The "limma" package was used to identify DEGs by comparing the expression value between normal and OA synovial tissues.[17] The corresponding p-value of the gene symbols after the independent-samples *t*-test was defined as adjusted $p < 0.05$, and $|\log_2 FC| > 1.5$ were considered as screening criteria. The "ComplexHeatmap" package[18] and "ggplot2" package[19] were then used to make the complex heatmap and volcano plot to better visualize these DEGs.

Gene ontology, KEGG, and disease ontology analyses of DEGs. We used the "clusterProfiler" package to perform the GO and KEGG pathway enrichment analyses of DEGs.[20] A "GOplot" package was used to calculate the Z-score as well as visualize the results of these enrichment analyses.[21] Disease ontology (DO) enrichment analysis was performed and visualized by the online tool Enrichr (Icahn School of Medicine at Mount Sinai, USA). A p-value < 0.05 was considered statistically significant.

PPI network construction and identification of the hub genes. The PPI network was constructed using the STRING database with a filter condition (confidence score 0.4).[22] Then, Cytoscape (Institute for Systems Biology, USA) was used to better visualize the interaction information performed by STRING. Additionally, MCODE plugin was used to identify significant gene modules (degree cut-off = 2; node score cut-off = 0.2; k-score = 2; maximum depth = 100). The top eight genes were identified by the three algorithms including Degree, Maximal Clique Centrality (MCC), and Maximum Neighborhood Component (MNC) of

Table I. Information of selected microarray datasets.

Accession numbers	Platform	Samples		Mean age, yrs (SD)		Sex, n (male/female)		Source tissue	Attribute
		Normal	OA	Normal	OA	Normal	OA		
GSE55235	GPL96	10	10	N/A	N/A	N/A	N/A	Synovium	Test set
GSE55457	GPL96	10	10	51 (18.7)	72.4 (5.6)	8/2	2/8	Synovium	Test set
GSE55584	GPL96	0	6	N/A	73.2 (7.9)	N/A	0/6	Synovium	Test set
GSE12021	GPL96	9	10	50.2 (20.7)	71.9 (6.1)	7/2	2/8	Synovium	Validation set
GSE32317	GPL570	0	19 (10 early-stage and 9 end-stage)	N/A	62.3 (10.5) (early-stage)	N/A	8/2 (early-stage)	Synovium	Validation set
					69.1 (6.1) (end-stage)		5/4 (end-stage)		

Annotation: GPL96: [HG-U133A] Affymetrix Human Genome U133A Array; GPL570: [HG-U133_Plus_2] Affymetrix Human Genome U133 Plus 2.0 Array.
N/A, not available; OA, osteoarthritis.

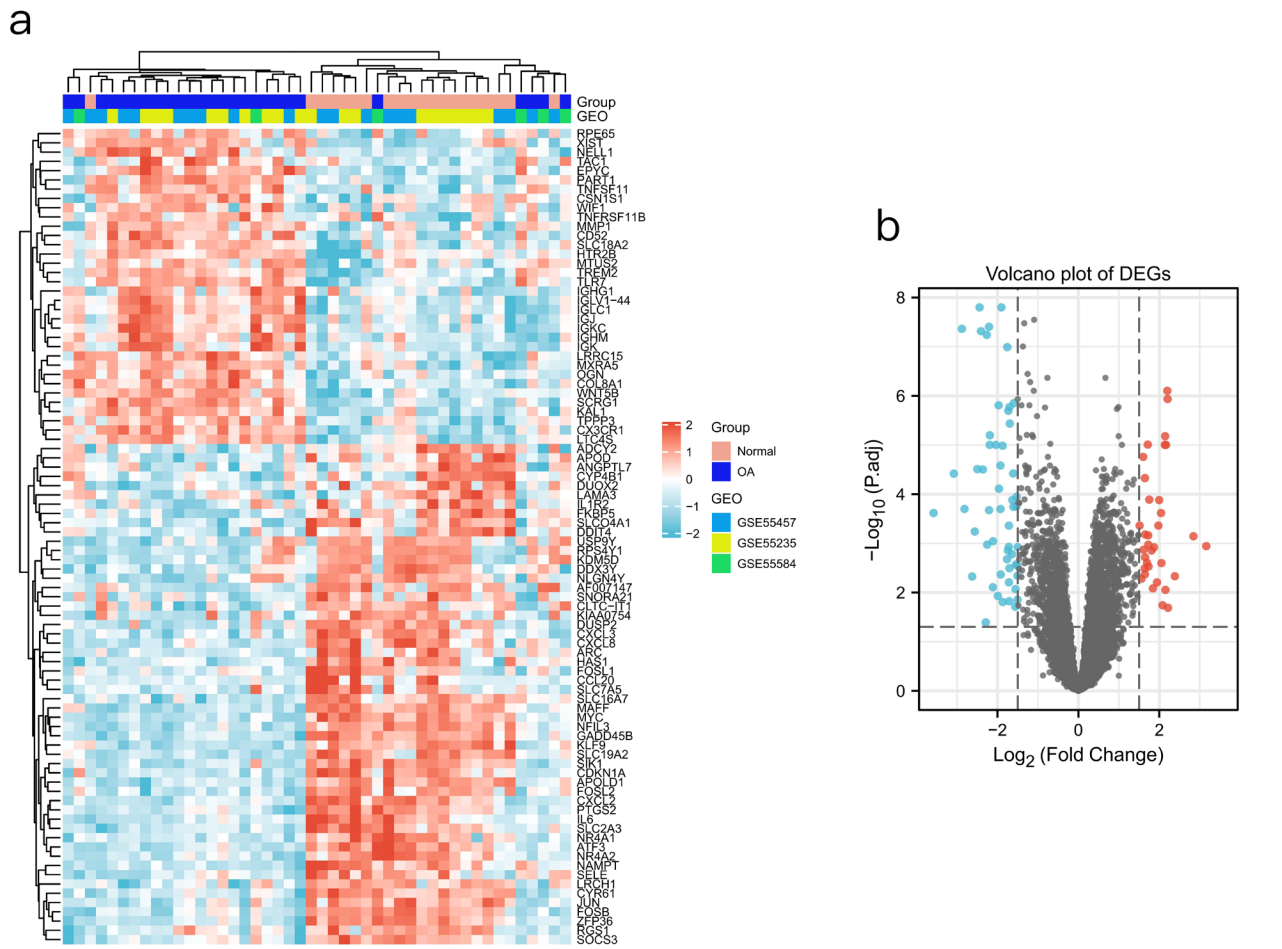

Fig. 1

Differentially expressed genes (DEGs) of synovial tissue between osteoarthritis (OA) and normal controls. a) Heatmap of DEGs. Red rectangles represent high expression, and blue rectangles represent low expression. b) Volcano plot of DEGs. Red spots represent upregulated genes, and blue spots represent downregulated genes.

CytoHubba.[23] Next, the top eight genes were verified by the support vector machine-recursive feature elimination (SVM-RFE) algorithm.[24] Finally, we intersected all these results to obtain the final hub genes. The GSE12021 dataset was analyzed to verify the hub genes of OA, while the GSE32317 dataset was analyzed to identify the significant differentially expressed genes between early-stage OA and end-stage OA.

Evaluation of immune cell infiltration. CIBERSORT (Stanford University, USA) was used to analyze the gene

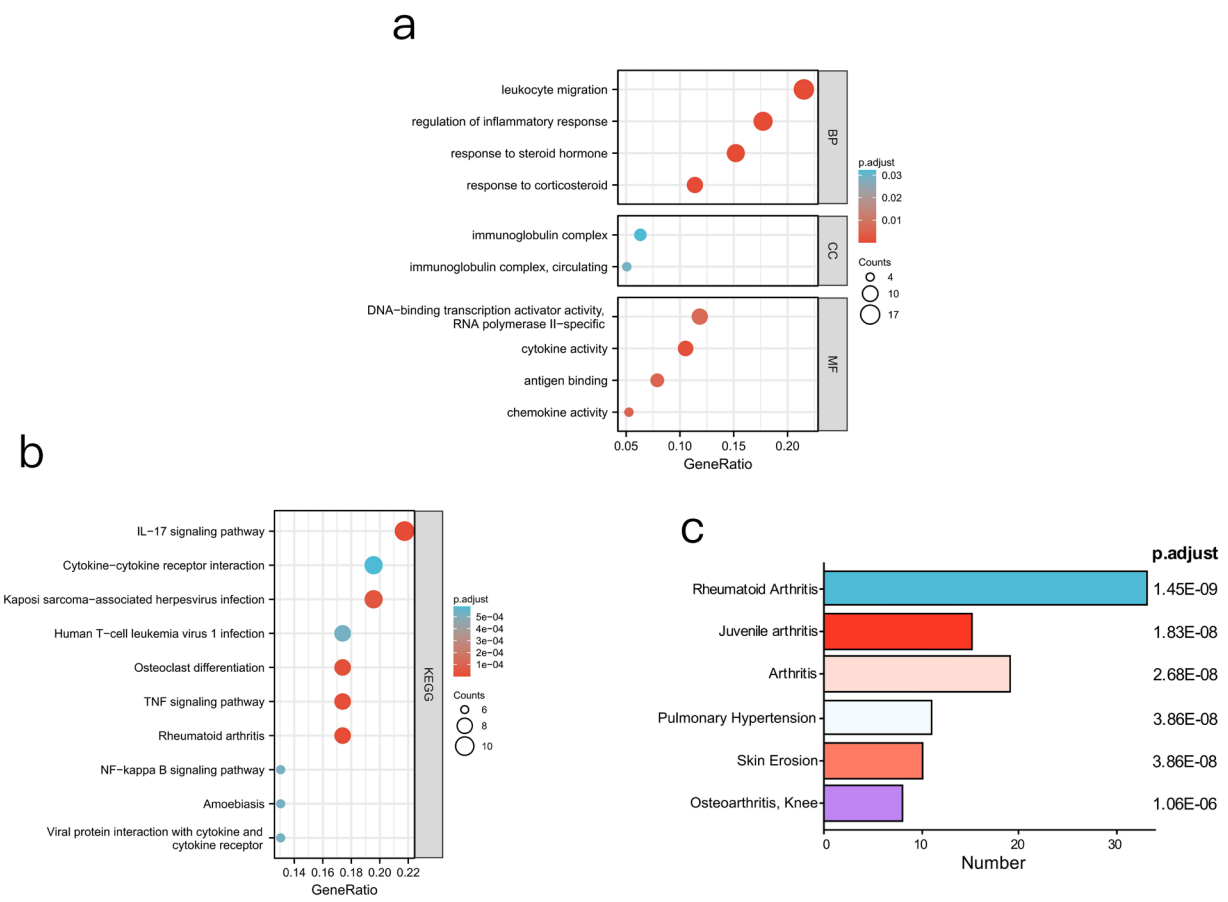

Fig. 2

Gene ontology (GO), Kyoto Encyclopedia of Genes and Genomes (KEGG), and disease ontology (DO) analyses of differentially expressed genes (DEGs) between osteoarthritis (OA) and normal controls. a) Bubble plot showing the top ten GO terms, including four biological processes, two cell components, and four molecular functions. b) KEGG pathway analysis of DEGs between OA and normal controls: the bubble plot shows the top ten enriched KEGG pathways of DEGs. c) Bar plot showing the DO enrichment analysis, where the horizontal axis represents the number of DEGs under the DO terms. IL-17, interleukin 17; NF-kappa B, nuclear factor kappa B; TNF, tumour necrosis factor.

expression matrix data obtained previously, and the samples were filtered out according to p-value < 0.05. Next, a percentage diagram of each kind of immune cell in every sample was made. Then the "ggplot2" package was used to draw a correlation heatmap which can visualize the correlation of infiltrating immune cells.[19] Next, the "ggplot2" package was used to visualize the different immune infiltration levels of each immune cell between early-stage OA and end-stage OA.

Correlation analysis between ATF3 and infiltrating immune cells. Finally, Spearman correlation analysis on ATF3 and infiltrating immune cells was performed using "ggstatsplot" package; "ggplot2" package was used to demonstrate the results.

Results

Identification of DEGs. To identify DEGs between OA and normal synovial tissue, the datasets GSE55235, GSE55457, and GSE55584 were selected. A total of 88 DEGs including 34 upregulated and 54 downregulated genes were detected. The results were visualized by a volcano map of all DEGs (Figure 1a), and a heatmap (Figure 1b) was made to show DEG expression.

Enrichment analyses of DEGs. GO enrichment analysis revealed that DEGs were mainly enriched in biological processes including leucocyte migration, regulation of inflammatory response, response to steroid hormone, and response to corticosteroid; cellular components including immunoglobulin complex and circulating immunoglobulin complex; and molecular functions including RNA polymerase II-specific DNA-binding transcription activator activity, cytokine activity, antigen binding, and chemokine activity (Figure 2a, Table II, Supplementary Figure a). KEGG enrichment analyses indicated that DEGs were mainly enriched in IL-17 signalling, cytokine-cytokine receptor interaction, osteoclast differentiation, and rheumatoid arthritis-related pathways (Figure 2b, Table II, Supplementary Figure b). DO analysis showed that diseases enriched by these DEGs mainly include rheumatoid arthritis, juvenile

Table II. The Gene Ontology and Kyoto Encyclopedia of Genes and Genomes enrichment analysis of differentially expressed genes.

Category	ID	Description	Gene count	Adjusted p-value	Genes
BP	GO:0050900	Leucocyte migration	17	4.88E-08	IGLV1-44, IGLC1, CXCL3, CXCL8, CXCL2, IL6, MMP1, CX3CR1, IGHM, CCL20, APOD, TNFSF11, TREM2, IGKC, SLC7A5, LRCH1, SELE
	GO:0050727	Regulation of inflammatory response	14	1.43E-05	IGLV1-44, IGLC1, IL6, PTGS2, APOD, TNFSF11, TREM2, TAC1, IGKC, SOCS3, IL1R2, TLR7, IGHG1, SELE
	GO:0031960	Response to corticosteroid	9	1.85E-05	FOSB, IL6, PTGS2, CSN1S1, KLF9, FOSL1, ZFP36, CDKN1A, DDIT4
	GO:0048545	Response to steroid hormone	12	3.75E-05	FOSB, NR4A1, IL6, PTGS2, CSN1S1, NR4A2, KLF9, KDM5D, FOSL1, ZFP36, CDKN1A, DDIT4
	GO:0032496	Response to lipopolysaccharide	11	4.60E-05	CXCL3, CXCL8, CXCL2, IL6, PTGS2, CX3CR1, TREM2, TAC1, ZFP36, JUN, SELE
CC	GO:0042571	Immunoglobulin complex, circulating	4	2.90E-02	IGLC1, IGHM, IGKC, IGHG1
	GO:0019814	Immunoglobulin complex	5	3.24E-02	IGLV1-44, IGLC1, IGHM, IGKC, IGHG1
MF	GO:0005125	Cytokine activity	8	1.17E-03	CXCL3, CXCL8, CXCL2, IL6, CCL20, TNFSF11, NAMPT, TNFRSF11B
	GO:0008009	Chemokine activity	4	5.48E-03	CXCL3, CXCL8, CXCL2, CCL20
	GO:0003823	Antigen binding	6	5.48E-03	IGLV1-44, IGLC1, IGHM, IGKC, SLC7A5, IGHG1
	GO:0001228	DNA-binding transcription activator activity, RNA polymerase II-specific	9	6.84E-03	FOSB, MAFF, NR4A1, ATF3, FOSL2, NR4A2, MYC, FOSL1, JUN
	GO:0042379	Chemokine receptor binding	4	9.18E-03	CXCL3, CXCL8, CXCL2, CCL20
KEGG	hsa04657	IL-17 signalling pathway	10	1.38E-08	FOSB, CXCL3, CXCL8, CXCL2, IL6, MMP1, PTGS2, CCL20, FOSL1, JUN
	hsa05323	Rheumatoid arthritis	8	3.55E-06	CXCL3, CXCL8, CXCL2, IL6, MMP1, CCL20, TNFSF11, JUN
	hsa04668	TNF signalling pathway	8	1.02E-05	CXCL3, CXCL2, IL6, PTGS2, CCL20, SOCS3, JUN, SELE
	hsa04380	Osteoclast differentiation	8	2.15E-05	FOSB, TNFSF11, TREM2, FOSL2, SOCS3, FOSL1, JUN, TNFRSF11B
	hsa05167	Kaposi sarcoma-associated herpesvirus infection	9	3.70E-05	CXCL3, CXCL8, CXCL2, IL6, PTGS2, MYC, ZFP36, JUN, CDKN1A
	hsa04061	Viral protein interaction with cytokine and cytokine receptor	6	5.20E-04	CXCL3, CXCL8, CXCL2, IL6, CX3CR1, CCL20
	hsa05146	Amoebiasis	6	5.20E-04	CXCL3, CXCL8, CXCL2, IL6, IL1R2, LAMA3
	hsa04064	NF-kappa B signalling pathway	6	5.20E-04	CXCL3, CXCL8, CXCL2, PTGS2, GADD45B, TNFSF11
	hsa05166	Human T-cell leukaemia virus 1 infection	8	5.25E-04	IL6, MYC, IL1R2, FOSL1, ZFP36, JUN, ADCY2, CDKN1A
	hsa04060	Cytokine-cytokine receptor interaction	9	5.87E-04	CXCL3, CXCL8, CXCL2, IL6, CX3CR1, CCL20, TNFSF11, IL1R2, TNFRSF11B

$p < 0.05$ was considered statistically significant.
BP, biological process; CC, cellular component; DEGs, differentially expressed genes; IL-17, interleukin-17; KEGG, Kyoto Encyclopedia of Genes and Genomes; MF, molecular function; NF-kappa B, nuclear factor kappa beta; TNF, tumour necrosis factor.

arthritis, arthritis, pulmonary hypertension, skin erosion, and OA (Figure 2c).

PPI network construction, module analysis, and identification of the hub genes. The PPI network, which was composed of 48 nodes and 192 edges, was constructed by STRING and visualized by Cytoscape (Figure 3). MCODE plugin was used to do the module analysis, and two cluster modules were obtained according to the filter criteria (Supplementary Figure c). Cluster 1 had the highest score (score: 6, 9 nodes and 24 edges), followed by cluster 2 (score: 3.692, 14 nodes and 24 edges). Then, three algorithms including MCC, MNC, and degree plugins were used to identify the top eight hub genes. After verifying and intersecting these hub genes with the SVM-RFE algorithm, we finally obtained six hub genes which are the most important genes in the interaction network, and may play a pivotal role in the pathogenesis of OA, including CXCL2, FOSB, JUN, ATF3, IL6, and CXCL8. Six hub genes with detailed information are shown in Table III.

Verification of six hub genes from the GEO dataset GSE12021. GSE12021, which included nine normal synovial samples and ten OA synovial samples, was selected to verify the six hub genes. The results are shown in Figure 4a, which indicate that the messenger RNA (mRNA) expression levels of the six hub genes in OA samples were significantly decreased compared with those in the normal samples ($p < 0.05$).

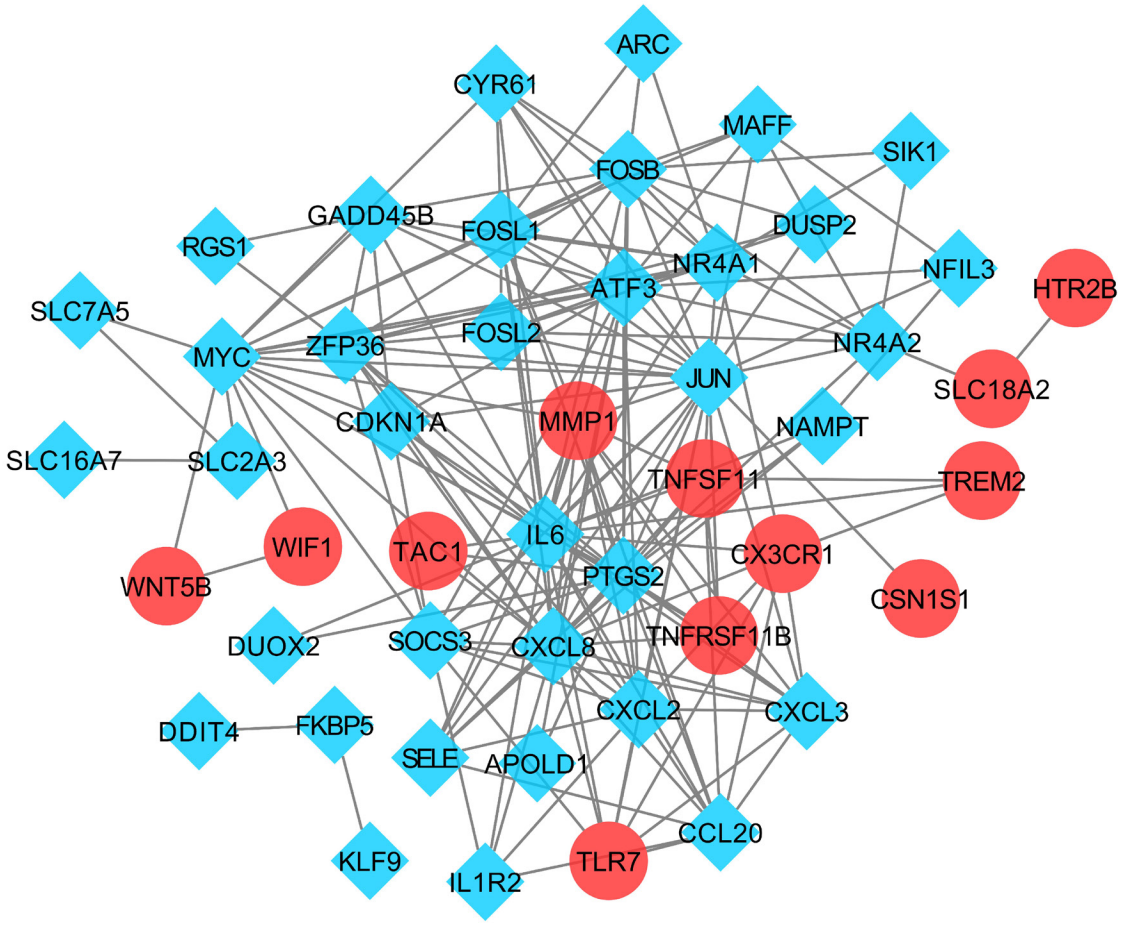

Fig. 3

Protein-protein interaction network of differentially expressed genes (DEGs). The interaction network between proteins coded by DEGs was constructed based on STRING database and Cytoscape software. ARC, activity regulated cytoskeleton associated protein; APOLD1, apolipoprotein L domain containing 1; ATF3, activating transcription factor 3; CCL20, C-C motif chemokine ligand 20; CDKN1A, cyclin dependent kinase inhibitor 1A; CSN1S1, casein alpha s1; CXCL8, C-X-C motif chemokine ligand 8; CXCL2, C-X-C motif chemokine ligand 2; CXCL3, C-X-C motif chemokine ligand 3; CX3CR1, C-X3-C motif chemokine receptor 1; CYR61, as known as CCN1, cellular communication network factor 1; DDIT4, DNA damage inducible transcript 4; DUOX2, dual oxidase 2; DUSP2, dual specificity phosphatase 2; FOSB, FosB proto-oncogene, AP-1 transcription factor subunit; FOSL1, FOS like 1, AP-1 transcription factor subunit; FOSL2, FOS like 2, AP-1 transcription factor subunit; FKBP5, FKBP prolyl isomerase 5; GADD45B, growth arrest and DNA damage inducible beta; HTR2B, 5-hydroxytryptamine receptor 2B; IL1R2, interleukin 1 receptor type 2; IL6, interleukin 6; JUN, Jun proto-oncogene, AP-1 transcription factor subunit; KLF9, KLF transcription factor 9; MAFF, MAF bZIP transcription factor F; MMP1, matrix metallopeptidase 1; MYC, MYC proto-oncogene, bHLH transcription factor; NAMPT, nicotinamide phosphoribosyltransferase; NFIL3, nuclear factor, interleukin 3 regulated; NR4A1, nuclear receptor subfamily 4 group A member 1; NR4A2, nuclear receptor subfamily 4 group A member 2; PTGS2, prostaglandin-endoperoxide synthase 2; RGS1, regulator of G protein signaling 1; SELE, selectin E; SIK1, salt inducible kinase 1; SLC16A7, solute carrier family 16 member 7; SLC18A2, solute carrier family 18 member A2; SLC2A3, solute carrier family 2 member 3; SLC7A5, solute carrier family 7 member 5; SOCS3, suppressor of cytokine signaling 3; TAC1, tachykinin precursor 1; TLR7, toll like receptor 7; TNFSF11, TNF superfamily member 11; TNFRSF11B, TNF receptor superfamily member 11b; TREM2, triggering receptor expressed on myeloid cells 2; WIF1, WNT inhibitory factor 1; WNT5B, Wnt family member 5B; ZFP36, ZFP36 ring finger protein.

Identification of the effective diagnostic markers of early OA. GSE32317, which included ten early-stage OA and nine end-stage OA samples, was used to identify the effective diagnostic markers of early OA. We observed that the mRNA expression level of ATF3 was significantly decreased in the end-stage OA samples compared with the early ones ($p < 0.001$, Figure 4b).

Receiver operating characteristic curve of six hub genes. We created the receiver operating characteristic (ROC) curves using the hub genes expression profiles of normal and OA samples in GSE12021, as well as the ROC curves of hub genes based on expression profiles of early-stage OA and end-stage OA samples in GSE32317 (Supplementary Figure d). Among the six hub genes, JUN has the highest diagnostic value (area under the curve (AUC) 0.988) in the OA samples, while ATF3 has the highest diagnostic value (AUC 0.975) in the end-stage OA samples. In order to identify better diagnostic markers, we combined the results of ROC curves with

Table III. Six hub genes identified by three algorithms of cytoHubba and support vector machine-recursive feature elimination.

Gene symbol	Description	Fold-change	Adjusted p-value	Regulation
CXCL2	C-X-C motif chemokine ligand 2	-2.499	3.09E-05	Down
FOSB	FosB proto-oncogene, AP-1 transcription factor subunit	-3.581	2.42E-04	Down
JUN	Jun proto-oncogene, AP-1 transcription factor subunit	-1.696	3.67E-06	Down
ATF3	Activating transcription factor 3	-2.189	6.34E-06	Down
IL-6	Interleukin-6	-2.256	1.06E-03	Down
CXCL8	C-X-C motif chemokine ligand 8	-2.561	5.75E-04	Down

SVM-RFE, support vector machine recursive feature elimination.

their expression levels; compared with end-stage OA, ATF3 was significantly upregulated in early-stage OA ($p < 0.001$). Therefore, ATF3 may have a high diagnostic value for early diagnosis of OA and could be a potential therapeutic target.

Immune cell infiltration analyses results. The landscape of immune cell infiltration in different stages of OA has not been fully elucidated. We first investigated the difference in immune cell infiltration between early-stage OA and end-stage OA tissues. The correlation heatmap revealed that M2 macrophages had a significant negative correlation with memory B cells ($p = 0.012$), plasma cells ($p = 0.017$), follicular helper T cells ($p = 0.038$), and activated NK cells ($p = 0.009$). Regulatory T cells (Tregs) had a significant negative correlation with follicular helper T cells ($p = 0.014$) and activated NK cells had a significant negative correlation with resting NK cells ($p < 0.001$), while resting mast cells also had a significant negative correlation with monocytes ($p = 0.011$). The plasma cells had a significant positive correlation with memory B cells ($p = 0.047$). M0 Macrophages had a significant positive correlation with activated NK cells ($p = 0.019$), while gamma delta T cells had a significant positive correlation with activated dendritic cells and resting mast cells ($p = 0.003$, Supplementary Figure e). The violin plot showed that several infiltrating immune cells varied significantly between early-stage OA and end-stage OA. Compared with early-stage OA tissue, end-stage OA tissue contained a lower proportion of resting NK cells ($p = 0.016$) and resting dendritic cells ($p = 0.043$), while plasma cells ($p = 0.043$) infiltrated more (Figure 5).

Correlation analysis between ATF3 and immune infiltrating cells. Correlation analysis (Figure 6) revealed that ATF3 was positively correlated with resting NK cells ($p = 0.034$, $|Cor| = 0.488$), resting dendritic cells ($p = 0.026$, $|Cor| = 0.510$), and regulatory T cells (Tregs, $p = 0.018$, $|Cor| = 0.535$).

Discussion

OA has become a common disease that brings substantial burdens not only to society but also to the healthcare system. However, because of the lack of early diagnostic biomarkers, once OA is diagnosed, it is always at the end phase of the disease, resulting in a poor prognosis. Moreover, in previous studies, cartilage was considered as the central component bearing the full brunt of the OA. Recently, more evidence indicated that OA is a whole-joint disease affecting entire articular tissues including cartilage, synovium, and subchondral bone.[25] Furthermore, during the development of OA, synovitis is always concomitant with OA from the early stage to the end stage.[26] It is reported that synovitis can lead to secondary OA by initiating cartilage degeneration and bone reconstruction.[27] In addition, researches also reveal that immune cell infiltration plays a vital role in the pathogenesis of OA.[12,14] Therefore, it is of great significance and urgency to clarify the underlying mechanism of OA and identify effective biomarkers for the early diagnosis of OA. In this study, we aimed to identify the effective markers for the early diagnosis of OA and explore the role of immune cell infiltration in OA.

Through functional analyses, the results indicate that inflammatory response, immune response, and synovial membrane signal transduction play an important role in OA, resulting in arthritis and pain, which are known as the main clinical manifestations of OA.[28] Additionally, the immune response may be related to infiltration of the immune cells, which needs to be further explored.

In this study, we found that ATF3 was significantly upregulated in early-stage OA with a high diagnostic value compared with end-stage OA. Therefore, we hypothesize that ATF3 may be an effective biomarker for the early diagnosis of OA based on our analysis. ATF3 is a member of the ATF/cyclic AMP response element-binding (CREB) protein family of transcription factors.[29] A couple of studies have indicated that ATF3 may play an important role in regulating the cell biological processes of the joint. Chan et al[30] reported that ATF3 can directly affect the transcription of matrix metalloproteinase (MMP)13. However, the increased expression of MMP13 would lead to the degradation of type II collagen, which could result in the loss of the extracellular matrix (ECM) and the imbalance of the cartilage homeostasis. Furthermore, IL-1β, which is considered to be related to the catabolic effects including growth inhibition and apoptosis induction of the chondrocyte, is reported to be mediated by ATF3.[31] All of these effects on cartilage would lead to bone remodelling in OA. Hence, we have reasons to believe that ATF3 is of great significance in maintaining the cells and joint function, as well as in the course of OA development. In addition, one study showed that the JNK/SAPK pathway is involved in the induction of ATF3, which indicated its potential role in stress responses.[32] Another study reported that ATF3 functions as a 'hub' of the cellular

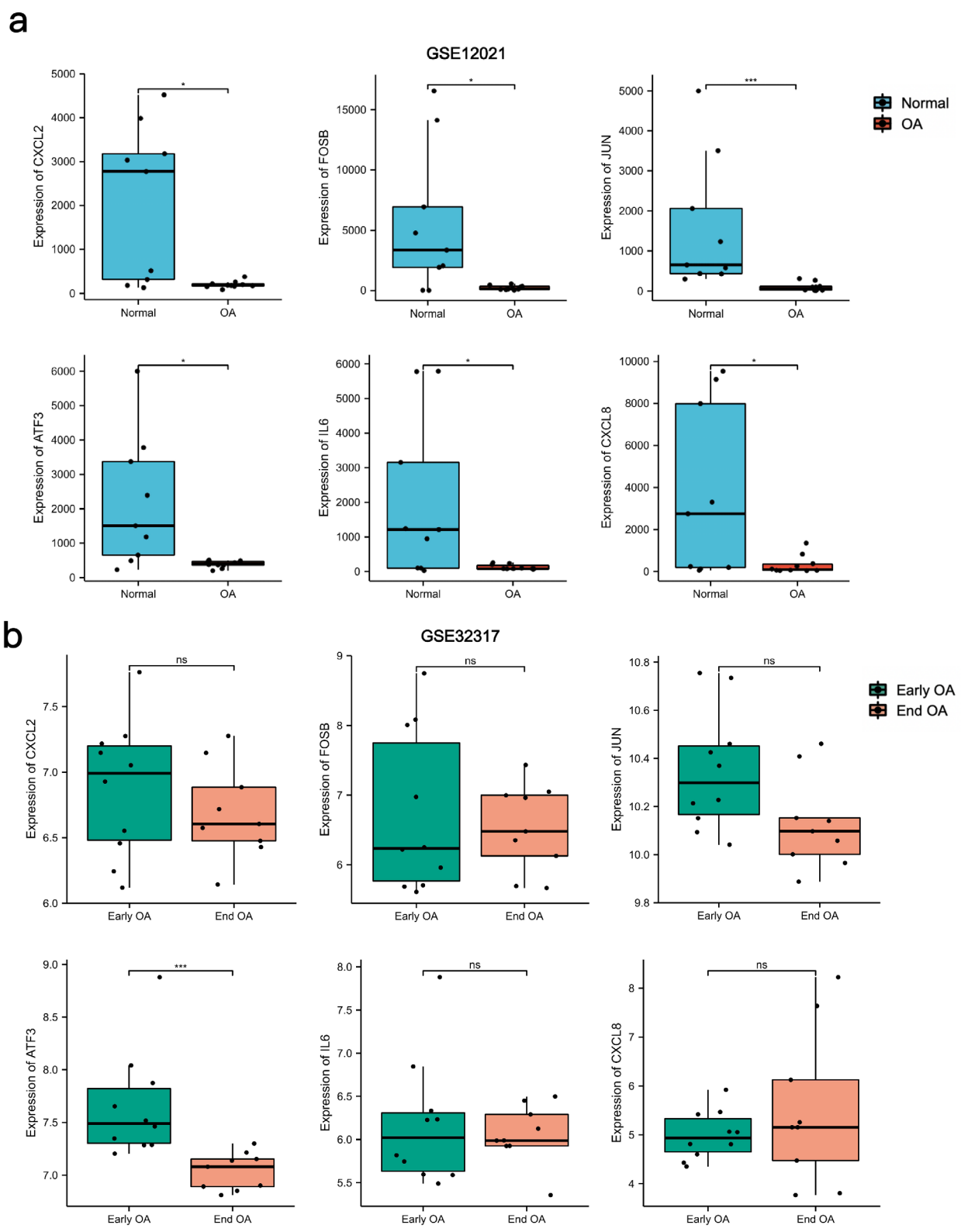

Fig. 4

Verification of the six hub genes by two datasets of the Gene Ontology database. a) Verification by GSE12021 (GPL96). Compared with normal controls, all hub genes were downregulated in osteoarthritis (OA) with significance. b) Verification by GSE32317 (GPL570). Compared with early OA, activating transcription factor 3 (ATF3) was downregulated in end-stage OA with significance, while others had no significance. ***p < 0.001; *p < 0.05; ns, no significant difference. CXCL2, C-X-C motif ligand 2; FOSB, FosB proto-oncogene, AP-1 transcription factor subunit; IL6, interleukin-6; JUN, Jun proto-oncogene; AP-1 transcription factor subunit.

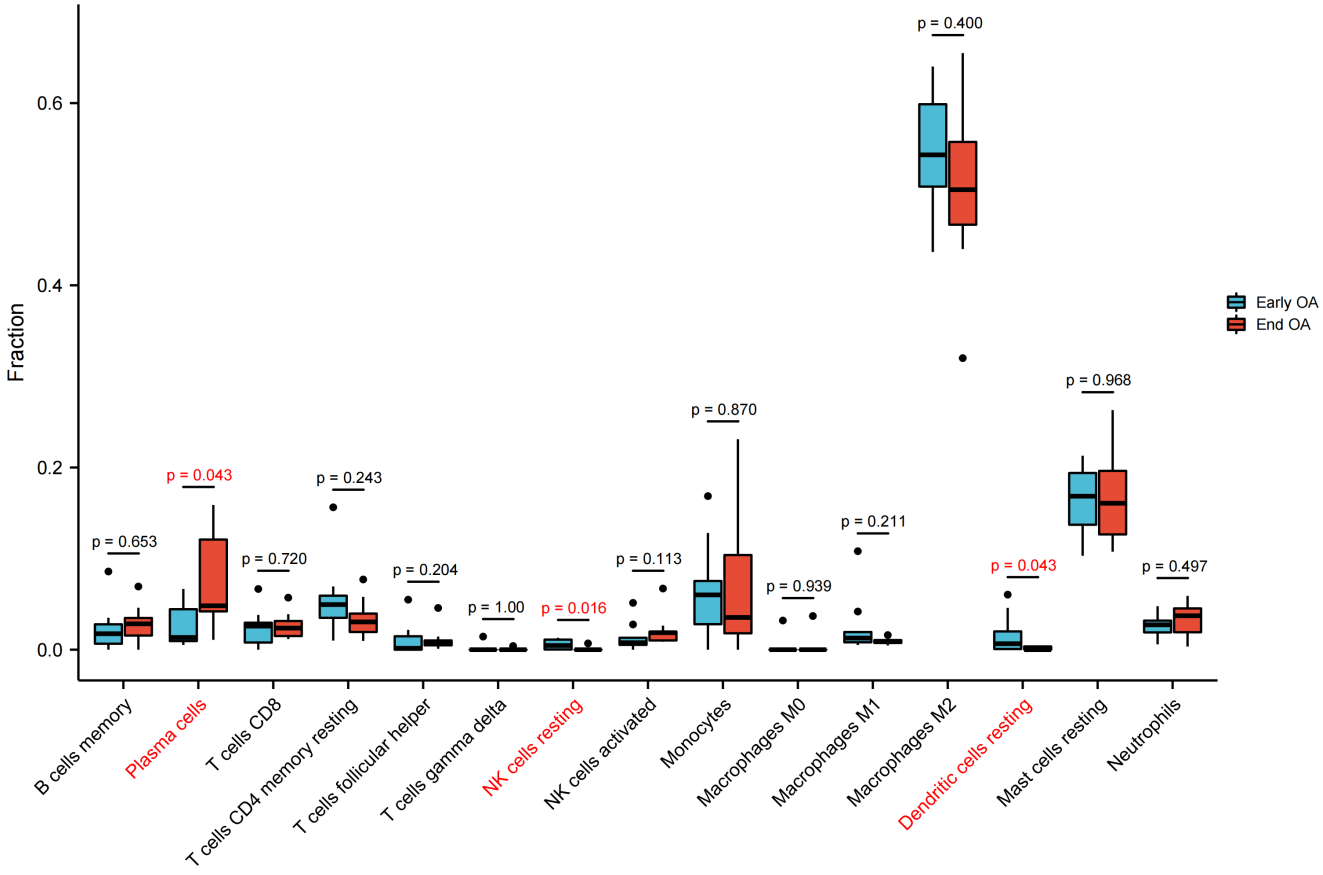

Fig. 5

Evaluation and visualization of the landscape of immune infiltration between early-stage osteoarthritis (OA) and end-stage OA. The difference of immune cell infiltration between early-stage OA and end-stage OA. The red marks represent the significant difference in infiltration between the two groups of samples. $p < 0.05$ was considered statistically significant. NK cells, natural killer cells. 'Fraction' refers to the proportion of each immune cell.

adaptive-response network, especially in the role of ATF3 in modulating inflammatory responses.[33] Moreover, a study showed that ATF3 is related to the regulation of cell growth, apoptosis, invasion, and collagen synthesis in keloid fibroblast through the transforming growth factor β (TGF-beta)/SMAD signalling pathway.[34,35] The roles of ATF3 in immunity, which may be related to Toll-like receptors, have also been reported.[36] In addition, during the literature search, we noticed that there may be some interactions between ATF3 and NF-kappa B1,[37] while manifestations of inflammation of synovial tissues in early-stage OA were associated with increased expression of NF-kappa B1.[38] Jiang et al[39] and Li et al[40] also found that ATF3 may be of great help to diagnose early-stage OA, and can be an effective therapeutic target. Therefore, we believe that ATF3 is likely to be involved in the pathogenic, immunological, and inflamed processes of OA. Furthermore, ATF3 is associated with some classic inflammation-related signalling pathways which play important roles in the progression of OA. However, more studies are still needed to fully reveal the roles of ATF3 in osteoarthritic synovial tissues.

As for immune cell infiltration in the development of OA, we found that plasma cells infiltrated significantly more while resting NK cells and resting dendritic cells infiltrated significantly less in end-stage OA, which may be related to OA progression. Previous studies have shown that OA patients often exhibit inflammatory infiltration of synovial membranes by plasma cells, NK cells, and dendritic cells.[41,42] One study revealed that biopsy samples from intensely inflamed synovium contained plasma cells.[43] Another study confirmed that NK cells play an important role in OA.[44] Further, a significant increase of dendritic cells has been observed in the synovial fluid of OA patients.[45] The literature above, combined with our analysis, indicates that the infiltration of plasma cells, NK cells, and dendritic cells may play crucial roles in OA development. However, further experimental evidence is needed to reveal the underlying mechanism. Our analysis also discovered some details of immune cell infiltration of OA, such as the finding that activated NK cells are significantly related to resting NK cells and M2 macrophages, while activated dendritic cells are significantly related to gamma delta T cells. As for the results of the correlation between ATF3 and immune cells, we

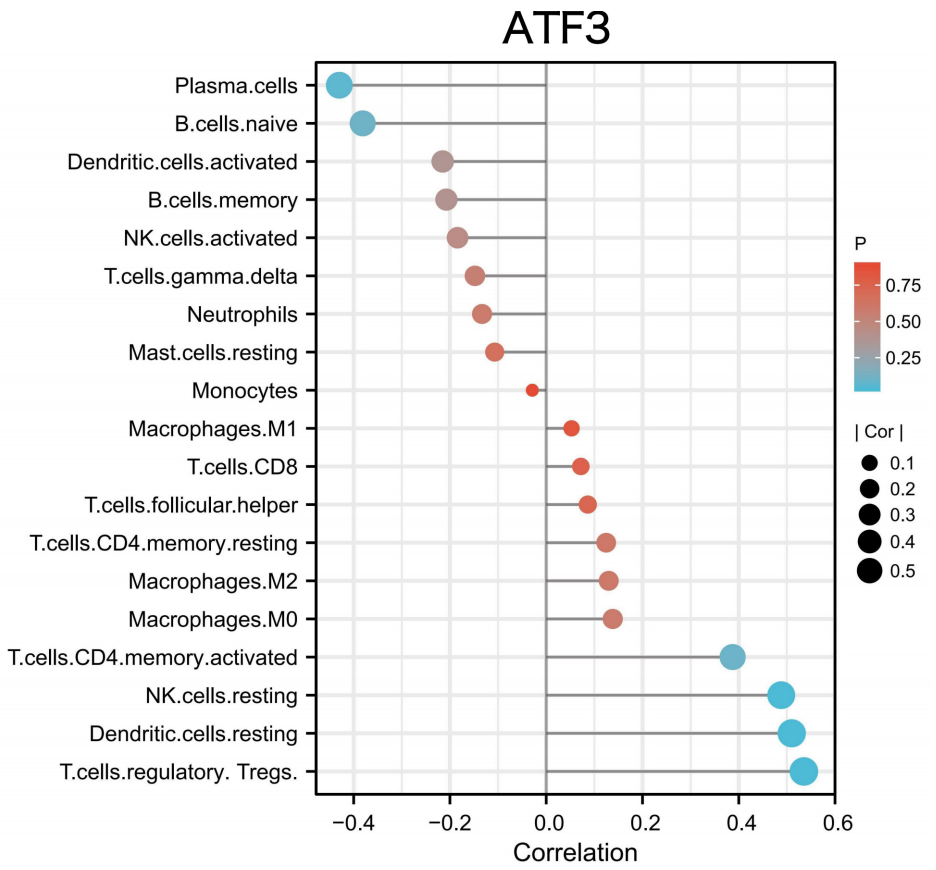

Fig. 6

Correlation between activating transcription factor 3 (ATF3) and immune infiltrating cells. The size of the dots represents the strength of the correlation between ATF3 and immune cells: the larger the dots, the stronger the correlation. The colour of the dots represents the p-value: the brighter shade of blue indicates a lower p-value. $p < 0.05$ was considered statistically significant.

hypothesize that ATF3 raises the number of NK cells, dendritic cells, and regulatory T cells, which are related to the occurrence and progression of OA. Our study found that ATF3 might correlate with immune cell infiltration and change the course of the development of the disease eventually, however all of these results require validation by cell and animal experiments; this can be the focus of further studies.

Despite some of the novel data-analyzing methods like SVM-RFE and CIBERSORT used, there are some limitations to our research. First of all, the sample size for analysis and verification is relatively small, which could result in the deviation of the hub genes and CIBERSORT analysis. In addition, it is reported that age and sex are considered to relate to OA prevalence.[46] However, some of the demographic information such as sex and age was missing from the selected datasets. The possible differences in the age and the sex distribution of the normal compared to OA samples might lead to unreliability in the results. Lastly, our analysis is based on previously published datasets. Although some previous studies are consistent with our results, the credibility of our results needs to be validated in further experiments.

To summarize, in our study we found that ATF3 may be a potential biomarker for the early diagnosis and treatment of OA. We also found that the differences in immune cell infiltration may be related to the differentially expressed ATF3 between early-stage OA and end-stage OA synovial tissue samples. Our study provides a theoretical basis and research direction for the early diagnosis, monitoring, and potential therapeutic intervention of OA.

Supplementary material

Figures showing more details about the osteogenesis of osteoarthritis (OA) and the role that activating transcription factor 3 plays in the development of OA, as well as its correlation with immune infiltration.

References

1. **Murphy CA**, **Garg AK**, **Silva-Correia J**, **Reis RL**, **Oliveira JM**, **Collins MN**. The meniscus in normal and osteoarthritic tissues: facing the structure property challenges and current treatment trends. *Annu Rev Biomed Eng*. 2019;21:495–521.
2. **Sanghani-Kerai A**, **Black C**, **Cheng SO**, **et al**. Clinical outcomes following intra-articular injection of autologous adipose-derived mesenchymal stem cells for the

treatment of osteoarthritis in dogs characterized by weight-bearing asymmetry. *Bone Joint Res.* 2021;10(10):650–658.
3. **He Z**, **Nie P**, **Lu J**, **et al**. Less mechanical loading attenuates osteoarthritis by reducing cartilage degeneration, subchondral bone remodelling, secondary inflammation, and activation of NLRP3 inflammasome. *Bone Joint Res.* 2020;9(10):731–741.
4. **Hunter DJ**, **Bierma-Zeinstra S**. Osteoarthritis. *Lancet.* 2019;393(10182):1745–1759.
5. **Chu CR**, **Williams AA**, **Coyle CH**, **Bowers ME**. Early diagnosis to enable early treatment of pre-osteoarthritis. *Arthritis Res Ther.* 2012;14(3):212.
6. **Dieppe PA**, **Lohmander LS**. Pathogenesis and management of pain in osteoarthritis. *Lancet.* 2005;365(9463):965–973.
7. **Jayadev C**, **Hulley P**, **Swales C**, **et al**. Synovial fluid fingerprinting in end-stage knee osteoarthritis: a novel biomarker concept. *Bone Joint Res.* 2020;9(9):623–632.
8. **Mathiessen A**, **Conaghan PG**. Synovitis in osteoarthritis: current understanding with therapeutic implications. *Arthritis Res Ther.* 2017;19(1):18.
9. **Guermazi A**, **Roemer FW**, **Hayashi D**, **et al**. Assessment of synovitis with contrast-enhanced MRI using a whole-joint semiquantitative scoring system in people with, or at high risk of, knee osteoarthritis: the MOST study. *Ann Rheum Dis.* 2011;70(5):805–811.
10. **Roemer FW**, **Guermazi A**, **Felson DT**, **et al**. Presence of MRI-detected joint effusion and synovitis increases the risk of cartilage loss in knees without osteoarthritis at 30-month follow-up: the MOST study. *Ann Rheum Dis.* 2011;70(10):1804–1809.
11. **Sellam J**, **Berenbaum F**. The role of synovitis in pathophysiology and clinical symptoms of osteoarthritis. *Nat Rev Rheumatol.* 2010;6(11):625–635.
12. **Ponchel F**, **Burska AN**, **Hensor EMA**, **et al**. Changes in peripheral blood immune cell composition in osteoarthritis. *Osteoarthr Cartil.* 2015;23(11):1870–1878.
13. **de Lange-Brokaar BJE**, **Ioan-Facsinay A**, **van Osch GJVM**, **et al**. Synovial inflammation, immune cells and their cytokines in osteoarthritis: a review. *Osteoarthr Cartil.* 2012;20(12):1484–1499.
14. **Rosshirt N**, **Hagmann S**, **Tripel E**, **et al**. A predominant Th1 polarization is present in synovial fluid of end-stage osteoarthritic knee joints: analysis of peripheral blood, synovial fluid and synovial membrane. *Clin Exp Immunol.* 2019;195(3):395–406.
15. **Davis S**, **Meltzer PS**. GEOquery: a bridge between the Gene Expression Omnibus (GEO) and BioConductor. *Bioinformatics.* 2007;23(14):1846–1847.
16. **Parker HS**, **Leek JT**, **Favorov AV**, **et al**. Preserving biological heterogeneity with a permuted surrogate variable analysis for genomics batch correction. *Bioinformatics.* 2014;30(19):2757–2763.
17. **Ritchie ME**, **Phipson B**, **Wu D**, **et al**. limma powers differential expression analyses for RNA-sequencing and microarray studies. *Nucleic Acids Res.* 2015;43(7):e47.
18. **Gu Z**, **Eils R**, **Schlesner M**. Complex heatmaps reveal patterns and correlations in multidimensional genomic data. *Bioinformatics.* 2016;32(18):2847–2849.
19. **Ginestet C**. ggplot2: elegant graphics for data analysis. *Journal of the Royal Statistical Society.* 2011;174(1):245–246.
20. **Yu G**, **Wang LG**, **Han Y**, **He QY**. clusterProfiler: an R package for comparing biological themes among gene clusters. *OMICS.* 2012;16(5):284–287.
21. **Walter W**, **Sánchez-Cabo F**, **Ricote M**. GOplot: an R package for visually combining expression data with functional analysis. *Bioinformatics.* 2015;31(17):2912–2914.
22. **No authors listed**. STRING Database. STRING Consortium. 2022. https://string-db.org/cgi/about (date last accessed 8 August 2022).
23. **Chin CH**, **Chen SH**, **Wu HH**, **Ho CW**, **Ko MT**, **Lin CY**. cytoHubba: identifying hub objects and sub-networks from complex interactome. *BMC Syst Biol.* 2014;8 Suppl 4:S11.
24. **Suykens JAK**, **Vandewalle J**. Least squares support vector machine classifiers. *Neural Processing Letters.* 1999;9(3):293–300.
25. **Scanzello CR**, **Goldring SR**. The role of synovitis in osteoarthritis pathogenesis. *Bone.* 2012;51(2):249–257.
26. **Wang H**, **Wang Q**, **Yang M**, **et al**. Histomorphology and innate immunity during the progression of osteoarthritis: Does synovitis affect cartilage degradation? *J Cell Physiol.* 2018;233(2):1342–1358.
27. **Ayral X**, **Pickering EH**, **Woodworth TG**, **Mackillop N**, **Dougados M**. Synovitis: a potential predictive factor of structural progression of medial tibiofemoral knee osteoarthritis -- results of a 1 year longitudinal arthroscopic study in 422 patients. *Osteoarthr Cartil.* 2005;13(5):361–367.
28. **Haviv B**, **Bronak S**, **Thein R**. The complexity of pain around the knee in patients with osteoarthritis. *Isr Med Assoc J.* 2013;15(4):178–181.
29. **Hai T**. The ATF Transcription Factors in Cellular Adaptive Responses. In: Ma J, ed. *Gene Expression and Regulation.* New York, NY: Springer, 2006: 329–340.
30. **Chan CM**, **Macdonald CD**, **Litherland GJ**, **et al**. Cytokine-induced MMP13 expression in human chondrocytes is dependent on activating Transcription Factor 3 (ATF3) regulation. *J Biol Chem.* 2017;292(5):1625–1636.
31. **Li X**, **Li Y**, **Yang X**, **et al**. PR11-364P22.2/ATF3 protein interaction mediates IL-1β-induced catabolic effects in cartilage tissue and chondrocytes. *J Cell Mol Med.* 2021;25(13):6188–6202.
32. **Hai T**, **Wolfgang CD**, **Marsee DK**, **Allen AE**, **Sivaprasad U**. ATF3 and stress responses. *Gene Expr.* 1999;7(4–6):321–335.
33. **Hai T**, **Wolford CC**, **Chang YS**. ATF3, a hub of the cellular adaptive-response network, in the pathogenesis of diseases: is modulation of inflammation a unifying component? *Gene Expr.* 2010;15(1):1–11.
34. **Wang XM**, **Liu XM**, **Wang Y**, **Chen ZY**. Activating transcription factor 3 (ATF3) regulates cell growth, apoptosis, invasion and collagen synthesis in keloid fibroblast through transforming growth factor beta (TGF-beta)/SMAD signaling pathway. *Bioengineered.* 2021;12(1):117–126.
35. **Duan M**, **Wang Q**, **Liu Y**, **Xie J**. The role of TGF-β2 in cartilage development and diseases. *Bone Joint Res.* 2021;10(8):474–487.
36. **Thompson MR**, **Xu D**, **Williams BRG**. ATF3 transcription factor and its emerging roles in immunity and cancer. *J Mol Med (Berl).* 2009;87(11):1053–1060.
37. **Zheng S**, **Abraham C**. NF-κB1 inhibits NOD2-induced cytokine secretion through ATF3-dependent mechanisms. *Mol Cell Biol.* 2013;33(24):4857–4871.
38. **Benito MJ**, **Veale DJ**, **FitzGerald O**, **van den Berg WB**, **Bresnihan B**. Synovial tissue inflammation in early and late osteoarthritis. *Ann Rheum Dis.* 2005;64(9):1263–1267.
39. **Jiang A**, **Xu P**, **Zhao Z**, **et al**. Identification of candidate genetic markers and a novel 4-genes diagnostic model in osteoarthritis through integrating multiple microarray data. *Comb Chem High Throughput Screen.* 2020;23(8):805–813.
40. **Li H**, **Yang HH**, **Sun ZG**, **Tang HB**, **Min JK**. Whole-transcriptome sequencing of knee joint cartilage from osteoarthritis patients. *Bone Joint Res.* 2019;8(7):290–303.
41. **Li YS**, **Luo W**, **Zhu SA**, **Lei GH**. T cells in osteoarthritis: alterations and beyond. *Front Immunol.* 2017;8:356.
42. **Pettit AR**, **Ahern MJ**, **Zehntner S**, **Smith MD**, **Thomas R**. Comparison of differentiated dendritic cell infiltration of autoimmune and osteoarthritis synovial tissue. *Arthritis Rheum.* 2001;44(1):105–110.
43. **Lindblad S**, **Hedfors E**. Arthroscopic and immunohistologic characterization of knee joint synovitis in osteoarthritis. *Arthritis Rheum.* 1987;30(10):1081–1088.
44. **Benigni G**, **Dimitrova P**, **Antonangeli F**, **et al**. CXCR3/CXCL10 axis regulates neutrophil-NK cell cross-talk determining the severity of experimental osteoarthritis. *J Immunol.* 2017;198(5):2115–2124.
45. **Alahdal M**, **Zhang H**, **Huang R**, **et al**. Potential efficacy of dendritic cell immunomodulation in the treatment of osteoarthritis. *Rheumatology (Oxford).* 2021;60(2):507–517.
46. **Liu Z**, **Wang H**, **Wang S**, **Gao J**, **Niu L**. PARP-1 inhibition attenuates the inflammatory response in the cartilage of a rat model of osteoarthritis. *Bone Joint Res.* 2021;10(7):401–410.

Author information:
- J. Yang, MBBS, Student
- Y. Fan, PhD, Orthopaedic Surgeon, Professor
- S. Liu, PhD, Orthopaedic Surgeon

Department of Orthopaedic Surgery, Peking Union Medical College Hospital, Chinese Academy of Medical Science, Beijing, China.

Author contributions:
- J. Yang: Software, Visualization, Formal analysis, Methodology, Writing – original draft.
- Y. Fan: Conceptualization, Supervision, Methodology, Writing – review & editing.
- S. Liu: Validation, Visualization, Writing – review & editing.

Funding statement:
- The authors received no financial or material support for the research, authorship, and/or publication of this article.

Acknowledgements:
- This study was the re-analysis based on the published data from GEO database. We would like to thank GEO database for the sharing of data. We also thank www.xiantao.love for the figure technology support.

Open access funding
- The open access funding for this manuscript was self-funded.